



Research on Automated Grinding Process for Composite Materials Based on Industrial Robot

Yuxiao Pu*, Lingyu Shen, Pin Zhang and Jinliang Wang

Princeton University, Princeton NJ 08544, USA Research Institute for Special Structures of Aeronautical Composites, AVIC, Jinan, China

*18262639318@163.com

Abstract. Grinding is a critical process in the production of electromagnetic functional structures. To improve the grinding quality of these structures and enhance the working environment, an automated grinding process for electromagnetic functional structures was studied based on an automated grinding unit. The influence of various parameters (spindle speed, robot moving speed, grinding normal pressure, grinding inclination angle) on the grinding quality was investigated. Finally, automated grinding of electromagnetic functional structures verified that this automated grinding unit can meet the relevant grinding index requirements.

Keywords: Electromagnetic Functional Structure; Composite Materials; Automated Grinding; Process Research.

1 Introduction

Electromagnetic functional structures are vital components for the aerodynamic performance of aircraft. Their surface quality significantly impacts the aircraft's mechanical properties; a smoother surface results in relatively lower drag during flight. Grinding is a key part in the production process of electromagnetic functional structures, affecting the service life, mechanical performance, and electromagnetic properties of the airframe's electromagnetic functional structures. Grinding is mainly divided into two types: one is profiling grinding, where the grinding quality affects product assembly interface thickness, opening dimensions, step gaps with the airframe frame, and related indicators involving stealth performance, cruising speed, and maneuverability; the other is grinding the substrate for functional coating spraying, where the grinding critically influences coating adhesion and product appearance quality.

Recent advancements in industrial robotics, computer vision, and sensor-based control have enabled automated finishing processes. Companies such as ABB, KUKA, and Fanuc have integrated force sensing and vision systems into robotic cells for polishing, grinding, and deburring [1]–[3]. However, the automated grinding of complex curved composite structures—particularly thin-skinned honeycomb sandwiches—remains

challenging due to path planning complexity, surface irregularity, and material sensitivity, which require advanced sensing and real-time control strategies[4]–[5].

2 Overall Technical Scheme for Automated Grinding Based on Industrial Robot

Considering the shape characteristics, dimensions, grinding precision, and working stroke requirements of the product family to be ground, this unit adopts an overall technical approach utilizing a single robot coordinated with a rotary table to achieve the main grinding motion, while the robot carries the end effector to perform the grinding process.

The automated grinding unit consists of nine parts: the main motion module, end effector, positioning and clamping module, automatic tool changing module, visual positioning module, detection module, dust removal module, and integrated control and programming module. The main motion module comprises the robot and the rotary table. The end effector consists of a force control device and a grinding head. See Figure 1.

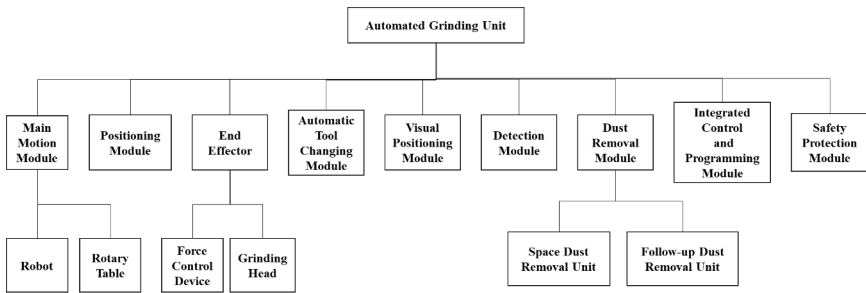


Fig. 1. Composition of Automated Grinding Unit

The main motion module is used to achieve the grinding motion during the process. The robot coordinates with the intermittent motion of the rotary table to meet the working stroke requirements for grinding radomes of different shapes and sizes. The end effector is installed at the robot's arm end to perform the product grinding. The force control device senses the grinding force applied by the grinding head on the product and maintains a constant grinding force through the automatic adjustment of the constant force mechanism [6]. The positioning and clamping module enables the quick positioning and clamping of workpieces/fixtures for different shaped and sized products on the rotary table. The automatic tool changing module, controlled by the grinding program, automatically changes corresponding specification grinding tools or detection devices. The visual positioning module establishes the coordinate relationship between the robot and the product. The detection module inspects the product's profile before and after grinding. The dust removal module is primarily used for the protection and collection of grinding dust, including a semi-enclosed space dust removal part and a follow-up dust removal part installed on the end effector. The safety protection module

prevents personnel entry during operation and supports the necessary operation of the control system in case of power failure or other abnormalities. The integrated control module is the brain of the entire grinding unit, performing data fusion with multiple sensors, completing the entire process from perception and decision-making to execution, ensuring the automation level of the grinding system. The automated grinding unit workflow is shown in Figure 2.

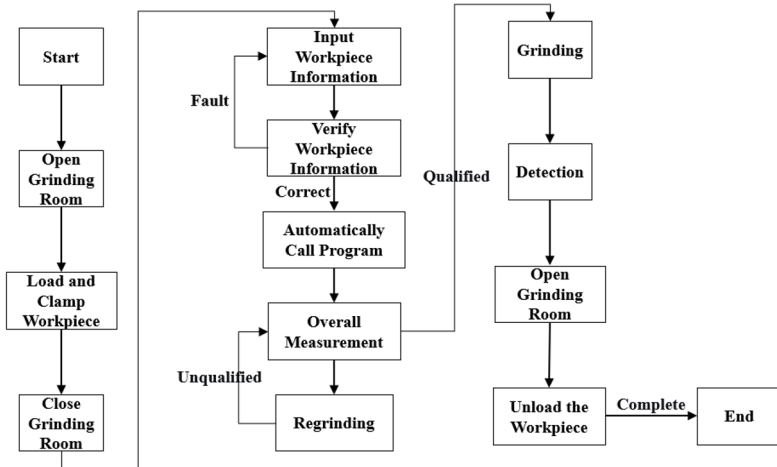


Fig. 2. Automated Grinding Unit Workflow

3 Research on Automated Grinding Process Scheme

Based on the automated grinding unit, research on the automated grinding process for electromagnetic functional structures was conducted, focusing on the influence of various automated grinding parameters (spindle speed, robot moving speed, grinding normal pressure, grinding inclination angle) on the surface condition of electromagnetic functional structures, to analyze and determine the optimal process parameters. Offline programming was implemented based on Robotmaster to achieve grinding path planning and grinding program writing.

For composite material radome test pieces, automated grinding process experiments were carried out using the automated grinding unit. By adjusting grinding parameters such as tool speed, feed rate, tool pressure, and forward tilt angle, the ground surfaces of the test pieces under different parameters were obtained. The surface morphology after grinding was observed and measured to analyze the influence of different processing parameters on the surface grinding of composite radomes.

3.1 Fixturing Scheme

Due to the limited workspace of the grinding robot, the rotary table is used to divide grinding stations to achieve full-surface grinding of the product. For axisymmetric-like

products, they are divided into 4 stations, i.e., 90° per station, completing the product grinding in four steps. For V-shaped and long strip products, they are divided into 2 stations, i.e., 180° per station, completing the product grinding in two steps.

During product fixturing, since the geometric center of the product cannot be guaranteed to lie on the axis of the rotary table, a separate workpiece coordinate system needs to be established for each grinding station to ensure the accuracy of the grinding path. The current coordinate system establishment method is manual alignment: a calibration block is fixed at a determined position on the grinding fixture, such as at a datum hole. The grinding disc of the robot end effector is replaced with a calibration pointer. The robot teach pendant is used to operate the robot to calibrate the origin of the workpiece coordinate system, a point on the positive X-axis, and a point on the positive Y-axis. The points selected for the positive X and Y directions should be as far as possible from the origin to minimize coordinate system calibration error. Currently, due to the size limit of the calibration block, the selected points are 100mm from the origin.

The accuracy of the current manual alignment method for coordinate system establishment is $\leq 1\text{mm}$. Taking the maximum value of 1mm, the axial deviation of the workpiece coordinate system is approximately 1° . Calculating for the maximum product diameter of $\phi 3000\text{mm}$, the coordinate system offset error at the farthest point is about 30mm. Considering the actual multi-station grinding process, the maximum distance from the origin during one grinding operation is 1500mm, resulting in a deviation of 15mm. The length of the end effector's force control device is $\pm 20\text{mm}$, which can still ensure compliant flexible grinding even under extreme conditions. Therefore, this coordinate system establishment method is feasible.

In the future, to further achieve automation, consider using a binocular vision camera to establish the coordinate system. The specific scheme involves setting more than 4 target points on the grinding fixture, using the binocular vision device to collect point position information, constructing the workpiece coordinate system, obtaining the transformation relationship between the workpiece coordinate system and the robot base coordinate system, thereby determining the positional relationship between the workpiece and the robot, and directly applying it to trajectory programming.

3.2 Offline Programming Scheme

The grinding path planning for the automated grinding unit adopts an offline programming approach, establishing the grinding path and automatically generating the grinding program. The specific steps are as follows:

Create a new workstation in Robotmaster software, call the KUKA KR210 robot model, and create the robot system based on the existing layout. Import the digital models of the test piece to be ground and the end effector into the workstation. After configuring the robot simulation environment, create the robot tool coordinate system and the test piece coordinate system.

Robot trajectory planning is divided into three parts: moving from the home position to the grinding start point, the grinding trajectory, and returning to the home position. For the selected sector area, a horizontal reciprocating trajectory is planned based on

the sector's shape. Determine parameters such as the start and end points of the grinding trajectory, grinding path spacing, spindle speed, robot moving speed, grinding pressure, and grinding inclination angle to generate the robot's automatic grinding trajectory. Through trajectory simulation, observe the robot's grinding path to determine the correctness of the trajectory planning, as shown in Figure 3. When the simulation meets the actual grinding requirements, the automatic grinding program can be generated.

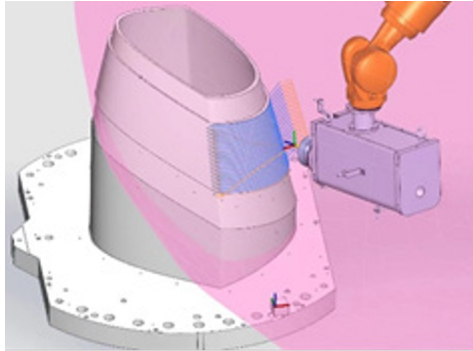


Fig. 3. Automated Grinding Path Planning

When planning the grinding path stepover, parameters of 5mm, 10mm, and 15mm were selected. Experimental verification showed that with a grinding inclination angle of 3° , a 5mm stepover yielded the best results, with the most uniform grinding surface and no missed areas.

When setting the connection between trajectories, either approach/retract methods or linear connection can be chosen. In actual grinding, since each approach impacts the product to some extent and the grinding amount at the approach position is larger, approach/retract motions should be minimized. Therefore, a linear connection method is used to transition directly to the next trajectory

3.3 Process Parameter Research Scheme

The grinding parameters for the automated grinding unit mainly include sandpaper grit, spindle speed, feed rate, grinding pressure, and grinding angle. Parameter process experiments were conducted based on the parameters of the current manual grinding method and previous research.

According to research, the sandpaper grit number used for manual skin grinding before painting is 120#, and the maximum speed of the pneumatic grinding tools used is 11000 rpm. However, the feed rate and grinding angle in manual grinding vary from person to person and change with different workpieces, so these two parameters need verification through process experiments. The grinding pressure test method involved using an electronic scale as a test tool, asking a skilled worker to grind on a flat plate placed on the scale, and recording the force variation during grinding. The test showed that the grinding force in manual grinding ranges between 20-30N. Subsequent grinding pressure for the automated unit will use this as a reference.

The grinding angle allows the outer edge area of the grinding disc with the highest linear speed to contact the surface to be ground, preventing the area near the center of the disc with lower linear speed from constantly contacting the product, which would result in poor grinding quality and overheating of both the disc and the product, as shown in Figure 4.

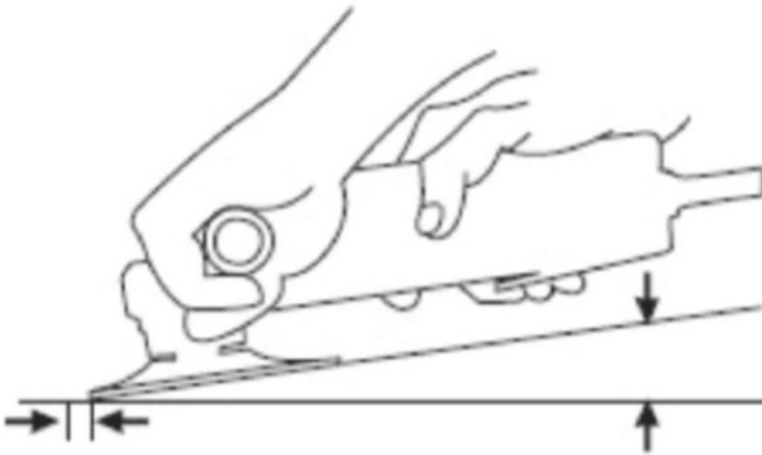


Fig. 4. Schematic Diagram of Grinding Angle

Spindle speed, feed rate, and grinding pressure mainly affect the grinding removal amount and efficiency. The relationship between these parameters and grinding quality is determined through comparative experiments, leading to the formulation of optimal process parameters.

3.4 Quality Characterization Research

To characterize the quality of the ground surface and confirm the grinding effect of the automated grinding unit, a grinding quality evaluation method needs to be established. Research indicates that surface roughness is a significant parameter affecting paint adhesion. Therefore, surface roughness is selected as the characterization parameter for grinding quality, and testing experiments are conducted.

After a skilled worker manually ground the product surface, a roughness measuring instrument was used to measure the ground areas. A total of 10 areas were selected. The measured surface roughness values ranged from Ra 0.927 to Ra 4.975. Because the composite material surface has a woven mesh structure, exhibiting anisotropy, the surface roughness value is a range. Currently, manual grinding relies on visual inspection, where a lack of gloss indicates qualification. Referencing the surface roughness of qualified products after manual grinding, the roughness reference value is tentatively set at Ra 1-5.

4 Process Application Verification

Grinding angle process experiments were conducted for the 125mm diameter grinding disc used in this automated grinding unit, with the test object being a flat plate test piece.

To prevent sandpaper damage, this experiment selected low speed, feed rate, and pressure, solely to observe the sandpaper condition after grinding. The selected parameters were 3000 rpm, 50 mm/s, pressure 5 lb, using a flat plate, with angles of 0°, 5°, and 10°.

The results showed that at 0°, the center of the sandpaper remained unused. Analysis attributed this to two reasons: the robot's own pose accuracy error and the coordinate system establishment error. At 10°, the inclination angle was too large, resulting in too small a contact area and material waste. At 5°, the angle was more suitable. Simultaneously, from the sandpaper structure, it can be seen that there are circular holes on the sandpaper exposing the grinding disc. This area should be avoided during grinding to prevent damage to the disc. Experimental verification showed that at 3°, the effective area of the sandpaper could be fully utilized.

Based on the grinding angle test results, industrial robot grinding parameter process experiments were carried out. The selected sandpaper was 120# grit, grinding angle 3°, spindle speeds selected were 6000 rpm, 8000 rpm, 10000 rpm, feed rates selected were 100 mm/s, 150 mm/s, 200 mm/s, grinding pressures selected were 5 lb, 6 lb, 7 lb, and the test object was a flat plate. The control variable method was used. The specific test content is as follows:

When other parameters remained constant, at spindle speeds of 6000 rpm, 8000 rpm, and 10000 rpm, scorching occurred on the flat plate surface. Analysis indicated that while the manual grinding tool (pneumatic grinder) has a maximum speed of 11000 rpm, the actual speed during contact with the workpiece does not reach 11000 rpm. Lacking professional equipment, the actual speed during grinding couldn't be measured accurately. Secondly, in manual grinding, the method involves quick reciprocating grinding over the same area, so the dwell time of the grinding disc at any specific location is relatively short. Based on the initial tests, the speed was reduced. It was found that speeds below 2000 rpm effectively suppressed scorching. Subsequently, speeds were adjusted to 500 rpm, 1000 rpm, and 1500 rpm for parameter testing. Results showed that 500 rpm was too low, resulting in poor grinding uniformity and low efficiency. When using 1500 rpm, scorching occasionally occurred. Therefore, to ensure grinding quality, a spindle speed of 1000 rpm was selected.

After determining the speed, feed rate parameter tests were conducted with the speed fixed at 1000 rpm. Results showed that feed rate had a minor impact on surface quality. However, at 200 mm/s, the approach speed was too fast, causing significant impact on the workpiece and excessive grinding at the entry point. At 100 mm/s and 150 mm/s, this phenomenon still occurred but was less severe. Therefore, to ensure workpiece grinding quality, a feed rate of 100 mm/s was initially selected, with plans to increase efficiency later while maintaining quality.

Finally, using parameters of 1000 rpm and 100 mm/s, the effect of grinding force on the surface was tested. Results showed that a 5 lb grinding pressure still caused excessive

removal, potentially damaging the skin. The grinding pressure was gradually reduced. At 1 lb pressure, the skin wasn't damaged, but grinding uniformity was poor. At 2 lb pressure, removal was excessive at the workpiece edges. Ultimately, a grinding pressure of 1.5 lb was selected.

Through the above experiments, the initial parameters for product grinding were determined as: 120# sandpaper, grinding angle 3° , spindle speed 1000 rpm, feed rate 100 mm/s, grinding pressure 1.5 lb. The following conclusions were drawn: Under otherwise constant conditions, higher spindle speed results in a smoother grinding surface; faster feed rate results in less grinding removal; greater grinding pressure results in more grinding removal.

These conclusions can be applied to subsequent process parameter optimization.

During process experiments, it was found that the grinding amount was excessive at the tool entry point. Analysis indicated that at entry, the spindle speed, feed rate, and grinding force were the same as during the main grinding process. However, due to the angled entry approach, the contact area between the grinding disc and the workpiece surface increases from small to large. The initial contact area is small, resulting in higher pressure per unit area and thus greater removal. If unresolved, this would cause over-grinding at the entry points during product grinding.

To solve the over-grinding at the entry point, a variable parameter grinding method was adopted. Specifically, separate grinding parameters are set for the entry point to reduce the grinding amount, while also reducing the entry angle to increase the initial contact area between the grinding disc and the product surface, thereby reducing pressure and achieving a smoother transition at entry. The parameters set for the entry point were: entry angle 30° , spindle speed 500 rpm, feed rate 50 mm/s, grinding pressure 1 lb. Test results proved this entry method feasible, as shown in Figure 5. The over-grinding phenomenon at the flat plate entry point was improved, ensuring uniform product grinding.



Fig. 5. Grinding Effect After Modifying Entry Parameters

5 Conclusions

This paper presents a computer-integrated robotic grinding system for electromagnetic functional composites. By combining binocular vision calibration, offline programming, and intelligent parameter control, the system achieves high precision, repeatability, and process automation. Automated grinding process research for electromagnetic functional structures was conducted based on an industrial robot automated grinding unit, focusing on the influence of robot offline programming and robot grinding parameters on grinding quality, thereby determining suitable automated grinding parameters. Finally, surface roughness was selected as the characterization parameter for grinding surface quality, a grinding scheme was formulated, product grinding process experiments were completed, and process application verification for pre-painting grinding of 3D curved composite products was achieved, proving the feasibility of the automated grinding unit's effectiveness. This grinding unit performs the grinding of electromagnetic functional structures automatically, overcoming the drawbacks of unstable quality and poor environment associated with traditional grinding methods. The process research in this paper holds reference value for discussing robot grinding of complex curved surfaces.

References

1. Xinlei D, Jinwei Q, Na L, et al. Robotic grinding based on point cloud data: developments, applications, challenges, and key technologies[J]. *The International Journal of Advanced Manufacturing Technology*, 2024, 131(7-8):3351-3371. DOI:10.1007/S00170-024-13094-W.
2. Anonymous. Unveiling the Future of Robotic Sanding and Polishing with Material Abrasion Technology[J]. *NASA Tech Briefs*, 2024, 48(4):S14-S17.
3. Jian L, Yonghong D, Yulin L, et al. A novel cascade calibration method for robotic grinding system[J]. *Intelligent Service Robotics*, 2024, 17(3):505-520. DOI:10.1007/S11370-024-00534-5.
4. Li Z, Li Y, Liu F, et al. Design, modelling, and implementation of a novel parallel end effector for robotic grinding[J]. *Robotics and Computer-Integrated Manufacturing*, 2026, 98103122-103122. DOI:10.1016/J.RCIM.2025.103122.
5. Yu C, Qiao J, Liu N, et al. Robotic grinding technology of multi-scale complex components based on 3D point clouds: a review[J]. *Measurement*, 2026, 257(PA):118663-118663. DOI:10.1016/J.MEASUREMENT.2025.118663.
6. Wang Z, Zou L, Wang W, et al. Cross-region robotic grinding with adaptive toolpath planning and force control for point clouds of complex curved workpieces[J]. *Journal of Manufacturing Systems*, 2025, 83856-877. DOI:10.1016/J.JMSY.2025.11.009

Open Access This chapter is licensed under the terms of the Creative Commons Attribution-NonCommercial 4.0 International License (<http://creativecommons.org/licenses/by-nc/4.0/>), which permits any noncommercial use, sharing, adaptation, distribution and reproduction in any medium or format, as long as you give appropriate credit to the original author(s) and the source, provide a link to the Creative Commons license and indicate if changes were made.

The images or other third party material in this chapter are included in the chapter's Creative Commons license, unless indicated otherwise in a credit line to the material. If material is not included in the chapter's Creative Commons license and your intended use is not permitted by statutory regulation or exceeds the permitted use, you will need to obtain permission directly from the copyright holder.

